Journal of Agricultural Engineering

https://www.agroengineering.org/

Dynamic calibration of broiler apparent temperature using real-time panting rate and machine learning: a pilot study

Yongmin Guo,[1*] Yali Ma,[1,2*] Changxi Chen,[1,2] Xiangchao Kong,[1,2] Deqi Hao,[1,2] Sai Luo[1,2]

[1]College of Computer and Information Engineering, Tianjin Agricultural University, Tianjin
[2]Key Laboratory of Smart Farming, Ministry of Agriculture and Rural Affairs, Tianjin, China

[*]*These authors contributed equally to this work and should be considered co-first authors*

Corresponding author: Xiangchao Kong, College of Computer and Information Engineering, Tianjin Agricultural University, Tianjin, China. E-mail: kxc_ouc@163.com

Please cite this article as doi: 10.4081/jae.2026.2110

Submitted: 19 January 2026
Accepted: 2 April 2026

Dynamic calibration of broiler apparent temperature using real-time panting rate and machine learning: a pilot study

Yongmin Guo,[1*] Yali Ma,[1,2*] Changxi Chen,[1,2] Xiangchao Kong,[1,2] Deqi Hao,[1,2] Sai Luo[1,2]

[1]College of Computer and Information Engineering, Tianjin Agricultural University, Tianjin
[2]Key Laboratory of Smart Farming, Ministry of Agriculture and Rural Affairs, Tianjin, China

[*]These authors contributed equally to this work and should be considered co-first authors

Corresponding author: Xiangchao Kong, College of Computer and Information Engineering, Tianjin Agricultural University, Tianjin, China. E-mail: kxc_ouc@163.com

Contributions: Yongmin Guo, investigation, formal analysis, writing – original draft; Yali Ma, investigation, data curation, validation, writing – original draft; Changxi Chen, methodology, software, visualization; Xiangchao Kong, conceptualization, supervision, project administration, funding acquisition, writing – review and editing; Deqi Hao, resources, software; Sai Luo, validation, writing – review and editing; Yongmin Guo and Yali Ma contributed equally to this work and should be considered co-first authors. All authors read and approved the final version of the manuscript and agreed to be accountable for all aspects of the work.

Conflict of interest: The authors declare that they have no known competing financial interests or personal relationships that could have appeared to influence the work reported in this paper.

Availability of data and materials: The datasets used and analyzed during the current study are available from the corresponding author on reasonable request.

Acknowledgements: This work was supported by the National Key Research and Development Program of China (Grant No. 2023YFD2000800); the China Agriculture Research System of the Ministry of Finance and the Ministry of Agriculture and Rural Affairs (Grant No. CARS-41); and the Young Scientific and Technological Talents Development Fund Program of Tianjin Agricultural University (Grant No. 2025QNKJ12). The authors would like to thank the editors and anonymous reviewers for their constructive comments and suggestions.

Abstract

To address the need for precise thermal environment assessment in intensive broiler farming, this study proposes a dynamic apparent temperature (AT) optimization model that incorporates

real-time biological feedback, overcoming the limitations of static traditional AT models. A baseline “AT-P” curve was established using the flock's minute-level panting rate (P) as a core biological feedback indicator. This curve is based on 7,138 records collected from a commercial farm, which include temperature, humidity, air velocity, age, and synchronously captured panting rate data. This curve maps observed panting to an “equivalent AT” representing the actual thermal load, with the deviation from traditional AT defined as the systematic correction residual. An Enhanced Attention Gradient Boosting Machine (EAG) ensemble model is then introduced to dynamically predict this residual, taking multi-source environmental features, traditional AT, and real-time panting rate as inputs, and outputting a corrected, optimized AT. Experimental results demonstrate that the EAG model achieves optimal performance in residual prediction, with an R^2 of 0.8329 and a mean absolute error (MAE) of 0.6503, significantly outperforming single base models and other mainstream algorithms. By integrating a static physical model with dynamic group behavioral feedback for online self-calibration, this study provides a methodological foundation for developing an animal-centric “perception-response-optimization” intelligent environmental control system in smart farming.

Key words: broilers; apparent temperature; panting rate; dynamic calibration; machine learning; smart farming.

Introduction

In modern intensive broiler farming, precise assessment of the thermal environment is critical for animal health and production efficiency (Cheng *et al*., 2024). Broiler physiological status depends not only on air temperature but also on a combination of factors, including humidity, air velocity, and radiation, which together define the “apparent temperature” (AT) (Olayiwola and Adedokun, 2025). Heat stress can reduce feed intake, impair growth, and suppress immunity, causing significant economic losses (Apalowo *et al*., 2024; Prates, 2025). Therefore, developing a dynamic index that accurately reflects the flock's thermal sensation in real time is a key scientific challenge. Research on quantifying environmental thermal effects has evolved through three stages. The first stage established fundamental physical evaluation indices. Houghton and Yaglou proposed “Effective Temperature” in 1923 (de Dear and Brager, 1998), which was later applied to animal husbandry (Mangan and Siwek, 2024). Building on this, AT was widely adopted for poultry house climate control due to its simplicity and adjustable

parameters (Brassó *et al*., 2025). By the end of the 20th century, research shifted toward dynamic environmental management.

The second stage explored the physiological and molecular mechanisms of heat stress. Modern broilers have inherent thermoregulatory limitations due to rapid muscle growth outpacing cardiopulmonary development. Studies have documented oxidative stress (Pečjak Pal *et al*., 2024), intestinal barrier damage (Khongthong *et al*., 2025), and immune dysfunction (Wang *et al*., 2025) induced by heat stress, providing biological rationale for AT-based models.

The third stage focuses on intelligent perception and feedback control based on animal ontology information, using sensors, computer vision, and machine learning to transform animal behavior into "biosensor" signals (Hernández-Sánchez *et al*., 2024; Neethirajan, 2022). Technologies such as infrared thermography (do Amaral Vercellino *et al*., 2025), vocalization analysis (Fan *et al*., 2025), and 3D visual monitoring (Italiya *et al*., 2025) have advanced rapidly (W. Ma *et al*., 2025). Nutritional interventions, including guanidinoacetic acid (Hernández-Sánchez *et al*., 2024) and probiotics (Hashemitabar and Hosseinian, 2024), have become important means to alleviate heat stress (Yehia *et al*., 2025).

Despite significant progress, a "logical gap" remains. On one hand, AT is inherently a static physical model, struggling to adapt to different flocks and transient microenvironments, leading to systematic deviation between "theoretical AT" and "biological thermal sensation" (Arias *et al*., 2023). On the other hand, behavioral feedback data have not been systematically used to calibrate AT models online, and a closed-loop system connecting environmental monitoring and animal response is lacking (Oso *et al*., 2025).

To bridge this gap, this study proposes a dynamic AT optimization model using real-time panting rate as a biological feedback signal, achieving for the first time closed-loop integration and online self-calibration of a static AT model with dynamic group behavioral feedback. By synchronously acquiring environmental data and video data, we analyze the relationships between environmental factors and broiler behavior and growth performance. This model retains the easy integration of traditional AT while gaining biological self-adaptability, providing a methodological foundation for developing perception-response-optimization smart farming environmental control systems.

Materials and Methods

Data Ccollection

The data for this study were collected at the Simate Farm 1 in Pingyuan County, Dezhou City, Shandong Province, China (GPS coordinates: 37.17°N, 116.44°E), with WOD168 white-feathered broilers as the research subjects. Data collection took place from June 12 to July 20, 2023, covering one complete rearing cycle. The poultry house was a mechanically ventilated enclosed building, measuring 101 meters in length, 16 meters in width, with an eave height of 4.2 meters and a ridge height of 6 meters, resulting in an internal volume of approximately 8241.6 cubic meters. The experiment was conducted with WOD168 white-feathered broilers over a complete production cycle from 1 to 39 days of age. A multi-tier cage rearing system was employed inside the house, with multiple rows of multi-level cages arranged. Each house contained 8 rows of cages, with 73 cage units per row and 4 tiers per unit.

Data collection primarily included two categories: first, internal environmental parameters of the poultry house, comprising indoor temperature (T), relative humidity (RH), air velocity (V), and carbon dioxide concentration (CO_2). These parameters were measured using a temperature and humidity sensor (model: RS-WS-N01-2-B-V9, temperature measurement range: -20℃ to +50℃, accuracy: ±0.2℃; humidity measurement range: 0–100% RH, accuracy: ±2% RH), a carbon dioxide sensor (model: RS-CO2-N01-V9, measurement range: 300–5000 ppm, accuracy: ±50 ppm), and an air velocity sensor (model: RS-CFSFX-N01-3H-V9, measurement range: 0.1–5 m/s, accuracy: ±(0.2 m/s ± 0.02v)), all manufactured by Shandong Renke Measurement and Control Technology Co., Ltd. Second, synchronized video stream data of the broilers were collected to record flock behavior and growth status. These video data were connected to a broiler panting rate calculation model for real-time computation of the per-minute panting rate. The panting rate calculation model employed the OM-YOLO algorithm (Y. Ma *et al*., 2025), enabling high-precision calculation of broiler panting rates (Cardoen *et al*., 2025). Descriptions of the original data fields are presented in Table 1.

All data were collected under consistent facility conditions, breed, and management protocols, ensuring data consistency and reproducibility.

Data preprocessing

Data cleaning

This step aimed to remove invalid or anomalous data segments caused by non-environmental or non-physiological factors that could interfere with model learning. The specific cleaning rules were as follows:

1) Equipment Failure Periods: Data from periods identified as equipment malfunctions were removed. This included sensor readings that were clearly outside physically plausible ranges (e.g., temperature > 50°C or < 10°C, relative humidity > 100% or < 10%) or periods with no data variation for an extended duration.

2) Management Operation Periods: Based on farm management logs, data collected during and for a short period (e.g., 2 hours) after operations such as vaccination, group medication, bird transfer, or equipment maintenance were excluded. It should be noted that the rationale for excluding these data is not due to abnormal environmental parameters, but rather because these operations induce acute stress responses in the flock (e.g., reduced activity, huddling, startled behavior), which are driven primarily by human intervention rather than thermal load. During such operational periods, environmental parameters (temperature, humidity, air velocity) may remain within normal ranges, but the flock's behavioral responses no longer reflect the physiological regulatory mechanisms associated with heat stress. Therefore, excluding these data ensures the purity of the environment-behavior relationship, allowing the model to focus on thermal load-driven physiological responses rather than confounding interference introduced by management operations.

3) Extreme External Event Periods: Data from periods coinciding with extreme weather events, such as severe storms or persistent heavy rain, were excluded by cross-referencing external meteorological records. The severe fluctuations in the indoor environment and animal stress responses during such events are not representative of general conditions.

Invalid data identification and processing

In the raw data, numerous instances were identified where the panting rate (P) was precisely 0 for extended periods (e.g., several consecutive hours). Cross-validation with farm operation

logs and video source data confirmed that these periods corresponded to nighttime light-off periods in the house. During these times, infrared illumination might have been insufficient or video capture may have failed, preventing the computer vision model from effectively detecting birds, thus outputting invalid zero values rather than true physiological behavior data. Therefore, for the core behavioral indicator "Panting Rate (P)", we formulated and implemented specialized processing rules to address systematic bias caused by changes in data collection conditions. The specific steps were:

1) Data Labeling: For the panting rate time series, all data segments where the value was continuously 0 for a duration exceeding 30 minutes were identified.

2) Logical Validation: These segments were validated against corresponding temperature data (T and the baseline AT). If the environmental temperature was significantly above the comfort zone threshold for that age group (e.g., baseline AT > 25°C) while P remained persistently 0, it contradicted physiological principles of heat stress, confirming the data as invalid.

3) Manual Review and Removal: Automatically labeled anomalous periods were cross-checked with the farm's daily lighting schedule. Periods confirmed as light-off or video capture failure were entirely removed. This step eliminated false behavioral signals introduced by system limitations, ensuring the authenticity of the behavioral data used to construct the "AT-Panting Rate" baseline relationship.

Through the above procedures, data segments potentially contaminated by non-thermal disturbances—such as abnormal gas concentrations, human interventions, or extreme environmental events—were systematically excluded, ensuring that the remaining dataset predominantly reflects thermal-induced panting responses under routine production conditions.

Missing value imputation

For random, brief gaps in data (e.g., consecutive missing records not exceeding 5 points) caused by instantaneous sensor communication failures during valid data collection periods, linear interpolation of the time series was used for imputation. For larger data gaps resulting from the cleaning and removal procedures, no imputation was performed, ensuring that all data used for modeling were genuine and valid observations.

the systematic preprocessing workflow described above, a high-quality, consistent, and reliable dataset was obtained, effectively eliminating non-physiological interferences and false signals. After preprocessing, a total of 7,138 valid records remained. This dataset laid a solid foundation for the subsequent mining of empirical baselines and the training of machine learning models.

Data splitting and reproducibility

To train and evaluate the machine learning models, the 7,138 valid records were randomly split into training and test sets at an 80%/20% ratio, resulting in 5,710 samples for training and 1,428 samples for testing. A fixed random seed (seed=42) was used during the data splitting process to ensure experimental reproducibility. All models were trained on the training set, with the test set used solely for final performance evaluation.

It is important to note that the prediction task in this study is not a time series forecasting problem in the conventional sense. The model does not predict future values based on past observations. Instead, it uses contemporaneous input features (temperature, humidity, air velocity, age, panting rate, and their derived features) corresponding to the exact same time point as the target to predict the residual—the deviation between the equivalent AT (derived from observed panting rate) and the traditional AT. In other words, the model learns a mapping from current environmental and behavioral states to the current correction residual, rather than learning temporal dependencies across time steps.

Furthermore, several aspects of the methodological design inherently mitigate the potential impact of temporal autocorrelation: i) Data preprocessing removed periods of strong non-stationary autocorrelation associated with equipment failures, management operations, and extreme external events, resulting in a dataset more representative of steady-state conditions; ii) the construction of the AT-P baseline curve employed a sliding window along the AT axis with median aggregation, effectively decoupling the mapping from the original time series structure, and subsequent isotonic regression further smoothed the curve, making the baseline mapping a global statistical relationship largely independent of temporal dependencies; iii) the feature set contains no time-lagged variables (e.g., panting rate from previous minutes), so the model was not designed to exploit temporal autocorrelation; iv) the ensemble tree models (LightGBM and XGBoost) make decisions based on feature value thresholds rather than sequential

dependencies, making them less sensitive to local autocorrelation. Considering these factors, we believe that the actual impact of random splitting on model performance evaluation in this study is limited. Nevertheless, we acknowledge that random splitting in time-series data is a methodological consideration, which is further discussed in the Discussion section.

Base AT calculation

To establish a unified initial index for thermal environment evaluation, the AT formula incorporating age correction was first applied to all preprocessed raw data. The calculation formula is as follows:

$$AT = T - V \times K_v + (RH - RH_{target}) \times K_h \quad \text{(Eq. 1)}$$

The target humidity (RH_{target}), wind chill coefficient (K_v), and wet-heat coefficient (K_h) in the formula are adjusted according to the broiler age groups to account for differences in thermal sensitivity at various growth stages (Zheng *et al*., 2025): chicks have immature thermoregulation and are more sensitive to cold/heat stress; as age increases, birds gradually become more adaptable to environmental fluctuations. By adjusting coefficients in this age-stratified manner, the AT calculation more accurately reflects the flock's actual thermal comfort state, thereby providing a more precise basis for environmental control and ventilation management. This method, based on empirical data, effectively balances physiological realism and operational feasibility in commercial farming scenarios. The specific segmented values for the wind chill and wet-heat coefficients are shown in Table 2.

AT-P baseline curve construction

This step aimed to establish a biological response baseline that reflects the average relationship between “AT” and “Panting Rate (P)”, independent of specific instantaneous environmental combinations. First, all cleaned historical data were paired based on the calculated original baseline AT values and the original P values. According to physiological differences, the data were grouped by age (Age), and baseline curves were constructed independently within each group. Within each age group, a sliding window with a width of 0.5 AT units and a step size of 0.1 AT units was applied along the baseline AT axis. For each window, all data samples whose

baseline AT values fell within that window were captured. The median of the P values corresponding to these samples, denoted as P_m, was calculated as the "typical" behavioral response level for the window center AT_c. Using the median instead of the mean effectively resists interference from invalid data. For the dataset grouped by age, given a sliding window centered at c with width w, the calculation formula for its typical value (median) is as follows:

$$P_m(c) = Median\left(\left\{P_i \mid AT_i \in [c - \frac{w}{2}, c + \frac{w}{2}]\right\}\right) \quad \text{(Eq. 2)}$$

Where P_i and AT_i are the baseline AT value and panting rate value of the i-th sample within the window. The final output is a set of discrete data points representing the group's average response: (AT_{c_i}, P_{m_i}).

To ensure the constructed baseline conforms to the fundamental biological constraint that "heat stress response strengthens as AT increases", isotonic regression was applied for smooth fitting to the above discrete points. Specifically, the PAVA (Pool Adjacent Violators Algorithm), which is the standard algorithm for isotonic regression, was employed. This algorithm iteratively merges adjacent points that violate the monotonicity constraint and replaces them with weighted averages, efficiently producing an optimal fit that satisfies the monotonicity constraint. Isotonic regression was chosen over more flexible nonlinear alternatives (e.g., splines or LOESS) for three primary reasons. First, it enforces a monotonicity constraint that directly encodes the well-established biological prior that increasing thermal load should not lead to a decrease in panting response, thereby preventing physiologically implausible oscillations in the fitted curve. Second, compared to unconstrained nonlinear smoothers, isotonic regression offers greater robustness against invalid data and reduces the risk of overfitting to noise, which is particularly important given the inherent variability in behavioral data collected under commercial farm conditions. Third, the resulting piecewise-constant or piecewise-linear fit provides a parsimonious and interpretable representation of the baseline relationship, facilitating stable inverse querying for equivalent AT calculation. While methods such as splines or Gaussian processes could capture more nuanced nonlinearities, they may inadvertently introduce non-monotonic artifacts that lack biological justification. The chosen isotonic regression thus strikes a balance between biological plausibility, statistical robustness, and computational efficiency for the subsequent baseline-dependent operations. Isotonic regression is achieved by solving

the following constrained optimization problem:

$$\min_{y_1,\ldots,y_N} \sum_{i=1}^{N} (y_i - P_m(c_i))^2$$
$$\text{subject to } y_1 \le y_2 \le \ldots \le y_N \qquad \text{(Eq. 3)}$$

Where y_i is the fitted function value at c_i. After fitting, a continuous baseline curve is obtained through interpolation, denoted as $P_{base} = f(AT)$.

Visual inspection of the fitted curve against the original discrete points confirmed that the monotonic constraint was well satisfied, with the curve smoothly tracking the central tendency of the discrete points across the AT range, indicating that the baseline provides a biologically plausible and robust representation of the monotonic relationship between AT and panting rate for subsequent inverse querying.

To facilitate fast forward and reverse queries in subsequent steps, the smoothed curve was discretized into an ordered sequence of points and stored in a doubly linked list data structure. Based on this structure, two core functions were implemented:

AT_to_P(*AT*): input an AT value, locate its interval by traversing the linked list, and use linear interpolation to calculate and return the corresponding predicted baseline panting rate (P_{pred}). The specific formula is as follows:

$$P_{pred} = P_k + \frac{P_{k+1} - P_k}{AT_{k+1} - AT_k} \times (AT - AT_k)$$
$$AT_k \le AT \le AT_{k+1} \qquad \text{(Eq. 4)}$$

P_to_AT(*P*): input an observed panting rate, locate its corresponding interval on the curve by traversing the linked list, and use linear interpolation to inversely calculate an equivalent apparent temperature (AT_{eq}). The specific formula is:

$$AT_{eq} = AT_k + \frac{AT_{k+1} - AT_k}{P_{k+1} - P_k} \times (P - P_k)$$
$$P_k \le P \le P_{k+1} \qquad \text{(Eq. 5)}$$

This “equivalent apparent temperature” can be interpreted as: under the current observed level of flock behavioral response (P), the thermal load the flock is experiencing is equivalent to a standard AT value of AT_{equiv}.

The entire baseline curve establishment process is illustrated in Figure 1.

Residual calculation

To establish a machine learning model capable of dynamically correcting traditional thermal environment indices, it is necessary to provide it with a supervised signal with clear physical meaning. This step calculates the residual for each historical data sample based on the constructed "AT-P" empirical baseline curve, thereby quantifying the prediction deviation of the traditional AT model under actual comprehensive conditions.

Specifically, for the i-th sample in the dataset with observed values (T_i, RH_i, V_i, A_i, P_i), the following steps are taken. First, the observed original panting rate P_i for this sample is input into the reverse query function of the empirical baseline curve to obtain the corresponding equivalent apparent temperature, denoted as $AT_{eq,i}$. This value reflects the actual perceived thermal load level of the flock given the current observed behavior. Second, the baseline apparent temperature value $AT_{base,i}$ for the same sample, representing the prediction of the traditional model, has already been calculated using Eq. 1 based on its original environmental data. Finally, the difference between the equivalent AT and the baseline AT is calculated and defined as the $Residual_i$ or sample $_i$. The specific formula is as follows:

$$Residual_i = AT_{eq,I} - AT_{base,i} \quad \text{(Eq. 6)}$$

This residual has a clear physical interpretation: if $Residual_i > 0$, it indicates that under the combined effects of the current temperature, humidity, air velocity, age, and flock behavior, the actual thermal load borne by the flock is higher than the estimate from the traditional AT model. If $Residual_i < 0$, it means the actual thermal load is lower than the traditional estimate. The residuals calculated from all samples constitute the target variable set used for the subsequent machine learning model training. Their essence is the systematic bias that the traditional model needs to correct after incorporating real-time behavioral feedback.

Feature set construction and standardization

The feature set for this experiment consisted of four parts: original environmental features (*T*, *RH*, *V*), original physiological feature (Age), original behavioral feature (*P*), and the original AT calculated by Eq. 1. To eliminate the influence of different units/scales, optimize subsequent algorithm performance, and ensure model training effectiveness, z-score standardization was

applied to this feature set:

$$z = \frac{x - \mu_{train}}{\sigma_{train}} \quad \text{(Eq. 7)}$$

Where x is any original feature value, μ_{train} and $_{train}$ are the mean and standard deviation of that feature calculated on the training set.

Standardization is a feature engineering step applied only during model training and prediction, and is not used in any physically meaningful calculations.

To further enhance the model's ability to predict thermal comfort residuals and capture nonlinear relationships and synergistic effects among features, systematic feature engineering was performed on the above original features to derive multiple categories of advanced features. The specific construction methods are as follows:

(1) Nonlinear Transformation Features: Squared terms (T^2, RH^2, V^2) and cubic terms (T^3, RH^3) were constructed for key environmental variables to capture nonlinear relationships between environmental factors and heat stress responses.

(2) Interaction Features: To characterize the synergistic effects among multiple environmental factors and behavioral indicators, the following interaction features were constructed:

T×RH, T×V, RH×V: reflecting the combined effects of temperature-humidity, temperature-wind, and humidity-wind;

T×P: interaction term between temperature and panting rate, used to capture the moderating effect of behavioral responses on heat load at different temperature levels;

AT×RH, AT×V: interactions between apparent temperature and humidity, and between apparent temperature and wind speed;

T×RH×V: three-way interaction term.

(3) Physically Meaningful Features: To incorporate domain knowledge in thermal environment assessment, the following features were constructed:

Heat index: $0.5\times(T+61.0+((T-68.0)\times1.2)+(RH\times0.094))$, integrating temperature and humidity to characterize perceived heat load;

Wind chill: $13.12+0.6215T-11.37V^{0.16}$, quantifying the cooling effect of wind speed on perceived temperature;

Temperature-humidity ratio: $T/(RH+1)$, used to measure the temperature-humidity balance;

Apparent temperature differences and ratios: $AT-T$, $AT/(T+1)$, $AT\times T$, used to characterize deviations of AT from actual temperature.

(4) Statistical Features:

Comfort index: $0.7T+0.2(100-RH)+0.1V$, an empirical indicator integrating temperature, humidity, and wind speed to quantify the thermal comfort level of the flock;

Thermal load: $T\times RH/100$, characterizing the intensity of heat and humidity load;

Z-score and rank features: For each core variable (T, RH, V, P, AT), standardized scores (z-score) and percentile ranks (rank) were calculated to eliminate dimensional effects and enhance model robustness to data distribution. Among these, $P_$rank represents the percentile rank of panting rate, reflecting the relative position of flock behavior in the historical distribution.

Residual prediction model construction

The data in this study exhibit multidimensional feature complexity, as residual prediction for thermal comfort involves complex nonlinear interactions among temperature, humidity, air velocity, age, and behavioral indicators. Concurrently, farming environment data contain certain noise and volatility, requiring models to possess good noise resistance and generalization capabilities. Furthermore, residual prediction needs to achieve sub-degree Celsius accuracy to effectively correct traditional thermal environment indices, posing high demands on model predictive capability. Practical application also necessitates a reasonable balance between accuracy and computational efficiency. Based on the characteristics of the research data and modeling requirements, this paper proposes a residual prediction model that integrates the LightGBM and XGBoost gradient boosting algorithms and incorporates a dynamic attention weighting mechanism. Named Enhanced Attention GBM (EAG), this model can effectively address the aforementioned challenges and is particularly suited for handling the complex regression problem in this study.

LightGBM algorithm

LightGBM (Light Gradient Boosting Machine) is an efficient gradient boosting framework proposed by Microsoft. It employs a histogram-based decision tree algorithm, discretizing

continuous features into discrete histogram bins (Figure 2). This method significantly reduces memory usage and accelerates the training process, especially suitable for handling continuous environmental variables in this study. It adopts a leaf-wise growth strategy (Figure 3), selecting the leaf node with the largest gain for splitting each time, which can achieve better accuracy with the same number of splits. It directly supports categorical features, avoiding the dimensionality explosion issue caused by one-hot encoding; the age group in this study can be directly input as a categorical feature. Furthermore, it supports parallel and distributed computing, making full use of multi-core CPU resources, offering advantages when processing large-scale farming data.

XGBoost algorithm

XGBoost (eXtreme Gradient Boosting) is another widely used gradient boosting framework. Its core advantages include: adding L1 and L2 regularization terms to the loss function of traditional gradient boosting, effectively controlling model complexity and preventing overfitting; using the second-order Taylor expansion of the loss function, leveraging second-derivative information to make the optimization process more precise and converge faster; possessing the ability to automatically learn the optimal splitting direction for missing values, providing good robustness for potential missing values in sensor data. The specific workflow is shown in Figure 4.

Enhanced attention GBM algorithm

The Enhanced Attention GBM algorithm integrates the LightGBM and XGBoost algorithms through a dynamic attention mechanism. After feature engineering and standardization, input features are fed in parallel into the two base models, LightGBM and XGBoost, for training and prediction. The predicted values from both base models are concatenated with the original standardized features to form a new feature vector. Ridge Regression is then used to learn the optimal weight allocation for each sample, forming a dynamic attention weighting mechanism. Finally, the residual prediction value is obtained through weighted fusion. This architecture not only combines the strengths of both base models but also achieves adaptive adjustment to different sample characteristics through the attention mechanism, demonstrating superior

performance in prediction accuracy, model robustness, and generalization capability. The specific workflow is shown in Figure 5.

Evaluation metrics

During model training, Mean Squared Error (MSE) was selected as the loss function to optimize model parameters by minimizing the average squared difference between predicted and true values. To comprehensively evaluate model performance during the testing phase, three commonly used regression evaluation metrics were adopted: Mean Absolute Error (MAE), Root Mean Squared Error (RMSE), and the Coefficient of Determination (R^2). The definition and calculation formulas for each metric are as follows:

1) Mean Squared Error (MSE)

MSE measures the average of the squares of the differences between predicted and true values. It is more sensitive to larger errors, and a smaller value indicates higher model prediction accuracy. The calculation formula is:

$$MSE = \frac{1}{N}\sum_{i=1}^{N}(y_i - \hat{y}_i)^2 \quad \text{(Eq. 8)}$$

2) Mean Absolute Error (MAE)

MAE represents the average of the absolute differences between predicted and true values. It intuitively reflects the magnitude of prediction errors and is not affected by the direction of the error. The calculation formula is:

$$MAE = \frac{1}{N}\sum_{i=1}^{N}(|\hat{y}_i - y_i|) \quad \text{(Eq. 9)}$$

3) Root Mean Squared Error (RMSE)

RMSE is the square root of MSE. It retains the unit of the error, making it easier to compare with actual values, and similarly imposes a higher penalty on larger errors. The calculation formula is:

$$RMSE = \sqrt{\frac{1}{N}\sum_{i=1}^{N}(\hat{y}_i - y_i)^2} \quad \text{(Eq. 10)}$$

4) Coefficient of Determination (R^2)

R^2 is used to evaluate the model's ability to explain the variation in the target variable. Its value range is generally [0,1], with values closer to 1 indicating a better model fit. The calculation formula is:

$$R^2 = 1 - \frac{\sum_{i=1}^{N}(y_i - \widehat{y_i})^2}{\sum_{i=1}^{N}(y_i - \overline{y_i})^2} \quad \text{(Eq. 11)}$$

Where N represents the number of samples, y_i represents the actual output value, $\widehat{y_i}$ is the model-predicted value, and $\overline{y_i}$ is the mean of the actual values.

Integration of the apparent temperature correction model

For new real-time observation data, the traditional baseline apparent temperature is first calculated based on the environmental data. Then, all features are input into the trained residual prediction model to obtain the predicted residual. Finally, the corrected AT is output.

$$AT_{Calibration,i} = AT_{Base,i} + Residual_i \quad \text{(Eq. 12)}$$

Results

Enhanced attention GBM training results

To comprehensively evaluate the performance of the thermal comfort residual prediction method, we established an experimental platform on an Ubuntu 18.04 system with Python 3.8. Using LightGBM and XGBoost as baseline models, the experiment employed a dynamic attention-weighted ensemble method to combine them, forming the new Enhanced Attention GBM model. Regarding randomness control: we fixed the random seeds for data splitting (seed=42), model initialization (seed=42), and data sampling (seed=42) to ensure experimental reproducibility. The Enhanced Attention GBM model adopted the following optimized parameter configuration: the number of trees was set to 300 to increase model capacity, the maximum depth was limited to 8 to prevent overfitting, the learning rate was set to 0.03 to balance convergence speed and accuracy, the subsample and feature sampling ratios were both set to 0.8 to enhance model robustness, and the regularization parameters (L1=0.1, L2=0.1) effectively controlled model complexity. To improve training efficiency, the model utilized all

available CPU cores for parallel training (n_jobs=-1), with Root Mean Squared Error (RMSE) serving as the core evaluation metric. The experimental results for the Enhanced Attention GBM model are presented in Table 3.

To further explore the influence of individual features on model predictions, feature importance ranking and partial dependence analysis were conducted on the trained Enhanced Attention GBM model, as illustrated in Figure 6.

Figure 6a presents the importance ranking of the top ten features, where the temperature-panting interaction term (T_P) has the highest weight (0.1848), followed by T_zscore and P_rank. Figure 6b shows the partial dependence plots for the six key features. According to the partial dependence plots, T_P exhibits a distinct threshold effect: when T_P is below approximately 1,500, the partial dependence remains near zero; above this threshold, it increases sharply in a nearly linear manner. This pattern suggests that the synergistic effect of elevated temperature and panting behavior becomes physiologically significant only after a certain combined intensity, likely corresponding to the activation of active heat dissipation mechanisms in broilers. T_zscore exhibits a sigmoid-like shape. When T_zscore is below approximately −0.5 (corresponding to temperatures below the thermal neutral zone), the partial dependence is slightly negative, indicating that the traditional apparent temperature model slightly overestimates the thermal load under cool conditions. When T_zscore exceeds 0, the partial dependence becomes positive and increases monotonically, reflecting the growing underestimation of thermal load by the static apparent temperature model under heat stress conditions. P_rank shows a gradual increase, with the slope steepening after P_rank exceeds approximately 0.7, indicating that panting behavior serves as a reliable indicator of heat stress primarily when the flock's panting prevalence surpasses a moderate baseline. P_zscore exhibits a similar pattern, with a near-flat region for values below 0.5 and a sharp increase beyond that point. T_RH displays a positive monotonic relationship, confirming that the combined effect of temperature and humidity contributes to increased thermal load beyond what is captured by the traditional apparent temperature model. Finally, the partial dependence plot for panting rate (P) alone shows a generally increasing trend, but the curve is less steep than that of the interaction features, suggesting that the predictive power of panting rate is enhanced when combined with temperature information.

Ablation study

To verify the effectiveness and necessity of the dynamic attention-weighted ensemble mechanism proposed in this study, we designed a systematic ablation study. This experiment compared the performance of the complete Enhanced Attention GBM model against its two independent base models—LightGBM and XGBoost—under identical experimental settings. The specific experimental results are shown in Table 4.

As shown in Table 4, the Enhanced Attention GBM model consistently outperforms both base models across all evaluation metrics. Figures 7 and 8 visually illustrate this model's advantages over the baseline models in terms of various metrics and the fit between predicted and true values.

Comparison with other models

To comprehensively and objectively evaluate the effectiveness and advancement of the proposed Enhanced Attention GBM model, this study conducted a horizontal comparison with various current mainstream machine learning regression models. The selected comparison models cover different algorithmic concepts and technical approaches, including the gradient boosting-based CatBoost, ensemble learning-based RandomForest, instance-based KNN, kernel method-based SVM, and probability inference-based BayesianRidge. This extensive comparison aims to verify that the proposed model not only outperforms its own components (as shown in the ablation study) but also maintains a competitive edge across a broader spectrum of algorithms. This demonstrates that its design possesses general superiority for the specific task of predicting broiler thermal comfort residuals, rather than being effective only within a specific model category. The specific results are shown in Table 5.

The comparison results indicate that the Enhanced Attention GBM model significantly outperforms all comparative models across all four evaluation metrics, demonstrating excellent comprehensive predictive performance. To present a more comprehensive and intuitive visualization of the Enhanced Attention GBM model's integrated performance advantages over other mainstream machine learning models, this study generated two sets of visual charts based on the numerical comparison table. These charts aim to transform abstract performance metrics into clear visual comparisons, thereby highlighting the proposed model's superior performance

across different dimensions, including prediction accuracy (R^2), error control (MSE, RMSE, MAE), and the degree of agreement between predicted and true values, as shown in Figures 9 and 10.

Discussion

This study proposed a dynamic apparent temperature correction model that integrates physical environmental data with group behavioral feedback. Experimental results demonstrate that the proposed Enhanced Attention Gradient Boosting Machine (EAG) model achieved optimal performance in the thermal comfort residual prediction task, demonstrating significant advantages over both individual base models and other mainstream algorithms. The following discussion systematically addresses the core contributions, methodological advantages, interpretability insights, and limitations with future directions.

By establishing a "behavior-equivalent AT" mapping relationship, this study effectively constructs a biological feedback feedforward channel, providing a data-driven solution to overcome the inherent "silent bias" of traditional environmental control systems based on fixed physical parameters. The findings indicate that fusing environmental and behavioral time-series data enables accurate quantification of the gap between biological thermal sensation and the physical environment. This approach aligns closely with the concept of "preventive welfare regulation"—predicting and proactively mitigating potential welfare risks by capturing early, subtle behavioral trends (e.g., dynamic changes in panting rate), rather than passively responding to already significant stress. Notably, the proposed dynamic calibration framework essentially transforms the broiler flock itself into a "biosensor", where real-time changes in respiratory behavior reflect the physiological cost of integrated environmental load. This perspective shift—from traditional "environment-centered" assessment to "animal-centered" perception—provides a new methodological foundation for intelligent environmental control systems.

At the algorithmic level, the dynamic attention-weighted ensemble strategy adopted in this study demonstrates significant advantages in handling the high noise, non-stationarity, and strong nonlinearity characteristic of agricultural field data. The ablation study confirms that this mechanism does not simply average base model predictions but dynamically integrates the

complementary strengths of LightGBM (excelling at efficient processing of sequential and categorical features) and XGBoost (possessing strong regularization to control model complexity) across different data subsets or feature patterns via attention weights. This "meta-learning" fusion strategy enhances model generalization and robustness in variable production environments. From a broader perspective, this approach addresses the classic dilemma in complex agricultural systems where "no single model fits all scenarios". Traditional physical models (such as the AT formula) perform well under specific conditions but struggle to adapt to dynamically changing microenvironments, while purely data-driven models may lose physical interpretability due to training data bias. By adopting a hybrid architecture of "physical baseline + data-driven residual", this study maintains the interpretable framework of physical models while endowing them with dynamic adaptability—a design philosophy with valuable implications for intelligent environmental control in agriculture.

Feature importance analysis and partial dependence plots together reveal the biological logic underlying model decisions. The interaction term between temperature and panting rate (T_P) ranks highest, confirming that the synergistic effect of environmental thermal load and physiological response is the primary driver of the residual between equivalent AT and traditional AT. The partial dependence plots further enrich interpretability: the threshold effect in T_P indicates a critical combined intensity for activation of active heat dissipation mechanisms; the sigmoidal shape of T_zscore reflects the typical thermal comfort zone and heat stress threshold for broilers; the steepening slope of P_rank after the 70th percentile suggests that the model effectively captures the transition from sporadic to sustained panting as a key indicator of significant heat stress. These threshold-based relationships not only validate the biological plausibility of the model's decisions but also highlight the value of incorporating dynamic behavioral feedback into thermal environment assessment. Importantly, the nonlinear relationships revealed by partial dependence plots—such as the negative partial dependence of T_zscore in the low-temperature range—identify systematic biases in the traditional AT model outside the thermoneutral zone, offering direct guidance for optimizing existing environmental control strategies.

Although this study, as a proof-of-concept, successfully demonstrates the feasibility of dynamically calibrating apparent temperature based on real-time behavioral feedback, several

limitations warrant further investigation. First, the singularity of data sources (single farm, one production cycle, one genetic line, one summer period) poses potential constraints on model generalizability. Different farms vary in ventilation system design, stocking density, and management practices; different seasons exhibit fundamentally distinct environmental parameter distributions; and different genetic lines differ in heat tolerance and physiological responses. Consequently, the "AT-P" baseline curve and EAG residual prediction model may, to some extent, be overfitted to the specific summer microclimatic patterns of this particular farm. Second, the data splitting approach employed random splitting rather than a time-series-based split, which theoretically poses a risk of temporal leakage. Although the prediction task is not a time series forecasting problem (the model uses contemporaneous inputs to predict contemporaneous outputs), and design elements such as baseline curve smoothing, the absence of lagged features, and data cleaning substantially mitigate the influence of temporal dependencies, the random splitting approach may still affect rigorous assessment of model generalizability to some extent. Third, while panting rate was employed as a key behavioral indicator of thermal load, it may also be influenced by non-thermal factors such as elevated carbon dioxide concentration, high stocking density, and sudden disturbances. Although this study minimized the potential impact of such confounders through rigorous data preprocessing—including exclusion of periods affected by management operations, equipment failures, extreme weather events, and nighttime light-off conditions—the residual influence of unmeasured non-thermal factors cannot be entirely ruled out. Fourth, the corrected apparent temperature has not been validated against independent physiological or performance indicators such as body temperature, feed intake, growth rate, mortality, or welfare indicators. The current study focuses on methodological feasibility, and whether the optimized AT more accurately reflects actual heat stress levels and can be associated with biologically meaningful outcome variables remains to be verified.

To address the above limitations, future research should systematically pursue the following directions: external validation across multiple farms, seasons, and genetic lines—including collecting year-round data from farms with different geographical locations and ventilation designs, incorporating data under diverse thermal conditions such as winter and transitional seasons, including different genetic lines (e.g., fast-growing vs. heat-tolerant strains), and

applying transfer learning or fine-tuning to verify model stability and reliability across different scenarios; adopting time-order-based splitting or time series cross-validation to obtain more robust generalization estimates; integrating multi-modal sensing technologies (e.g., CO_2, ammonia, acoustic signals) combined with controlled experiments to systematically disentangle the contributions of thermal and non-thermal stimuli to panting behavior; and systematically collecting concurrent physiological and performance data to quantify the incremental value of the corrected AT over traditional AT in predicting biological outcomes through correlation analysis or causal inference methods. Only through such comprehensive validation and improvement can the framework proposed in this study provide a truly universal methodological foundation for "perception-response-optimization" intelligent environmental control systems.

Conclusion

This study successfully developed an innovative framework that utilizes the real-time panting rate of broiler flocks as a biological feedback signal to dynamically correct apparent temperature through an Enhanced Attention Gradient Boosting Machine. This method effectively bridges the gap between traditional environmental physical models and the actual thermal sensation of animals. The core model (Enhanced Attention GBM), leveraging its dynamic ensemble mechanism, achieved predictive accuracy surpassing both individual models and various mainstream algorithms. Feature importance analysis not only validated the core driving role of the environment-behavior interaction effect but also provided interpretable biological insights into the model's decision-making. This study offers a practical technical solution and empirical foundation for promoting a paradigm shift in farming environmental control from "static formula-driven" to "dynamic biological feedback-driven", contributing a methodological basis for developing a smart livestock husbandry system centered on animal welfare.

References

Apalowo OO, Ekunseitan DA, Fasina YO, 2024. Impact of heat stress on broiler chicken production. Poultry 3:107-128.

Arias RA, Mader TL, Arias RA, 2023. Evaluation of four thermal comfort indices and their relationship with physiological variables in feedlot cattle. Animals (Basel) 13:1169.

Brassó LD, Komlósi I, Várszegi Z, 2025. Modern technologies for improving broiler production and welfare: a review. Animals (Basel) 15:493.

Cardoen T, de Carvalho PS, Antonissen G, Tuyttens FAM, Leroux S, Simoens P, 2025. Multi-camera detection and tracking for individual broiler monitoring. Comput Electron Agric 237:110435.

Cheng Q, Wang H, Xu X, He T, Chen Z, 2024. Indoor thermal comfort sector: a review of detection and control methods for thermal environment in livestock buildings. Sustainability 16:1662.

de Dear R, Brager GS, 1998. Developing an adaptive model of thermal comfort and preference. UC Berkeley, Center for the Built Environment. Available from: https://escholarship.org/uc/item/4qq2p9c6

do Amaral Vercellino R, de Alencar Nääs I, de Moura DJ, 2025. Tracking heat stress in broilers: a thermographic analysis of anatomical sensitivity across growth stages. Animals (Basel) 15:2233.

Fan W, Peng H, Yang D, 2025. Review: The application and challenges of advanced detection technologies in poultry farming. Poultry Sci 104:105870.

Hashemitabar SH, Hosseinian SA, 2024. The comparative effects of probiotics on growth, antioxidant indices and intestinal histomorphology of broilers under heat stress condition. Sci Rep 14:23471.

Hernández-Sánchez RC, Martínez-Castañeda FE, Domínguez-Olvera DA, Trujillo-Ortega ME, Díaz-Sánchez VM, Sánchez-Ramírez E, et al., 2024. Systematic review and meta-analysis of thermal stress assessment in poultry using infrared thermography in specific body areas. Animals (Basel) 14:3171.

Italiya J, Ahmed AA, Abdel-Wareth AAA, Lohakare J, 2025. An AI-based system for monitoring laying hen behavior using computer vision for small-scale poultry farms. Agriculture 15:1963.

Khongthong S, Piewngam P, Roekngam N, Maliwan P, Kongpuckdee S, Jeenkeawpleam J, et al., 2025. Effects of dietary Bacillus subtilis 14823 on growth performance, gut barrier integrity and inflammatory response of broilers raised in a stressful tropical environment. Poultry Sci 104:104518.

Ma W, Wang X, Tulpan D, Yang SX, Li Z, Zhao C, et al., 2025. Intelligent technologies in poultry farming: A review of smart breeding and precision production. Comput Electron Agric 239:111109.

Ma Y, Guo Y, Gao B, Zheng P, Chen C, 2025. Development of a tool to detect open-mouthed respiration in caged broilers. Animals (Basel) 15:2732.

Mangan M, Siwek M, 2024. Strategies to combat heat stress in poultry production—A review. J Anim Physiol Anim Nutr 108:576-595.

Neethirajan S, 2022. Automated tracking systems for the assessment of farmed poultry. Animals (Basel) 12:232.

Olayiwola SF, Adedokun SA, 2025. Heat stress in poultry: The role of nutritional supplements in alleviating heat stress and enhancing gut health in poultry. Front Vet Sci 12:1691532.

Oso OM, Mejia-Abaunza N, Bodempudi VUC, Chen X, Chen C, Aggrey SE, et al., 2025. Automatic analysis of high, medium, and low activities of broilers with heat stress operations via image processing and machine learning. Poultry Sci 104:104954.

Pečjak Pal M, Leskovec J, Levart A, Pirman T, Salobir J, Rezar V, 2024. Comparison of high n-3 PUFA levels and cyclic heat stress effects on carcass characteristics, meat quality, and oxidative stability of breast meat of broilers fed low- and high-antioxidant diets. Animals (Basel) 14:3314.

Prates JAM, 2025. Heat stress effects on animal health and performance in monogastric livestock: physiological responses, molecular mechanisms, and management interventions. Vet Sci 12:49.

Wang X, Chao X, Zhang W, Zhang X, Wu J, Ye C, et al. 2025. Heat stress influences immunity through dusp1 and hspa5 mediated antigen presentation in chickens. Animals (Basel) 15:1141.

Yehia M, Askri A, Achour A, Prus JMA, Ouellet V, Alnahhas N, 2025. Rectal temperature and heat transfer dynamics in the eye, face, and breast of broiler chickens exposed to moderate heat stress. Poultry Sci 104:104748.

Zheng P, Zhang W, Gao B, Ma Y, Chen C, 2025. Multi-step apparent temperature prediction in broiler houses using a hybrid SE-TCN–transformer model with Kalman filtering. Sensors (Basel) 25:614.

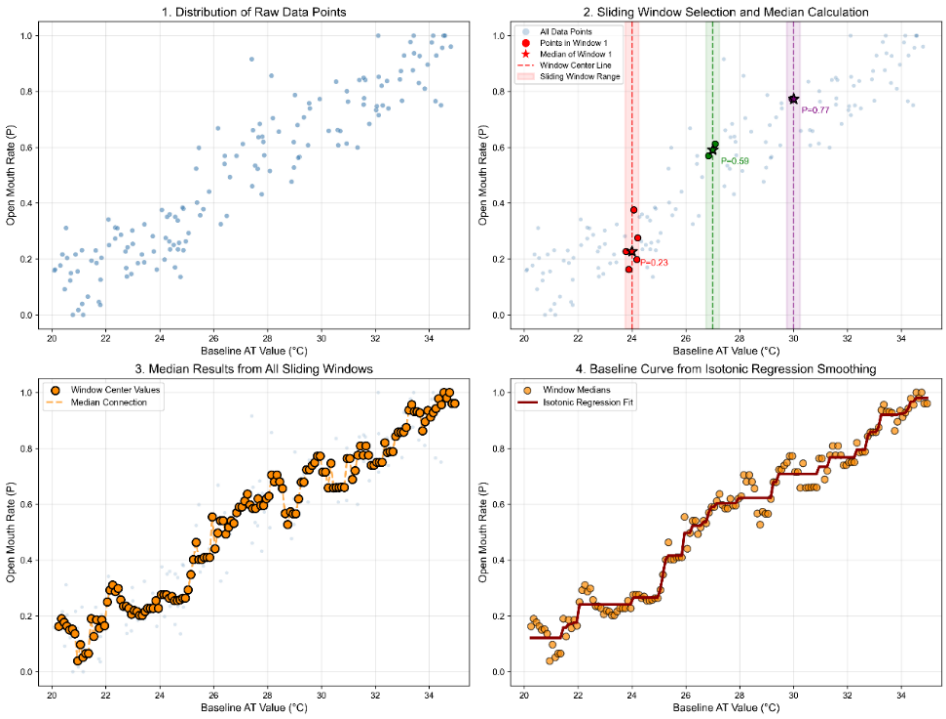

Figure 1. Baseline curve establishment steps.

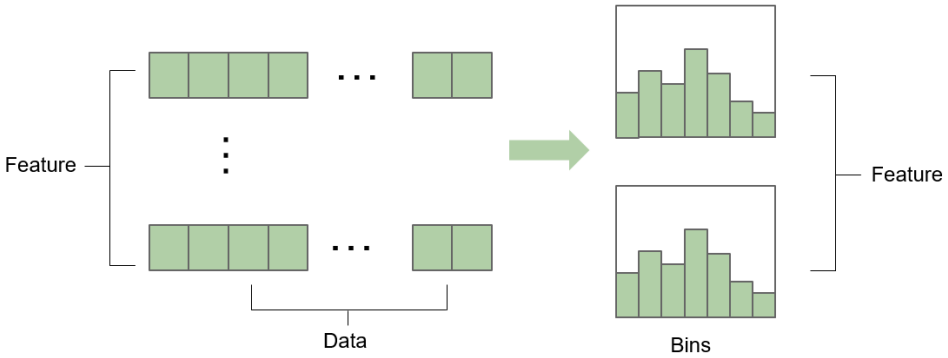

Figure 2. Histogram binning.

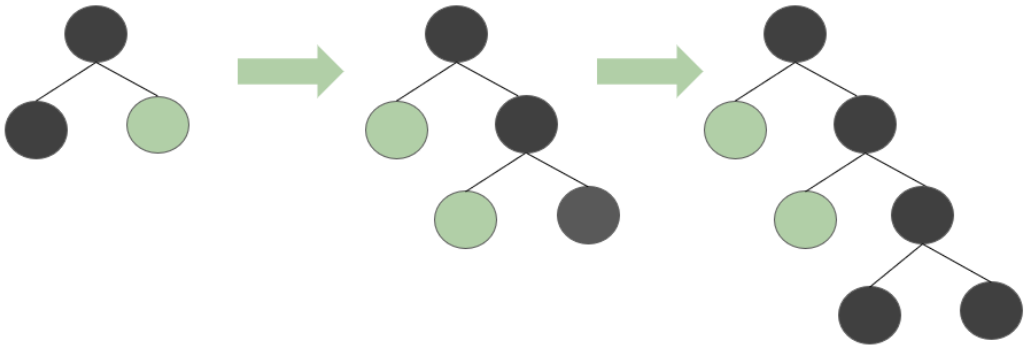

Figure 3. Leaf growth strategy.

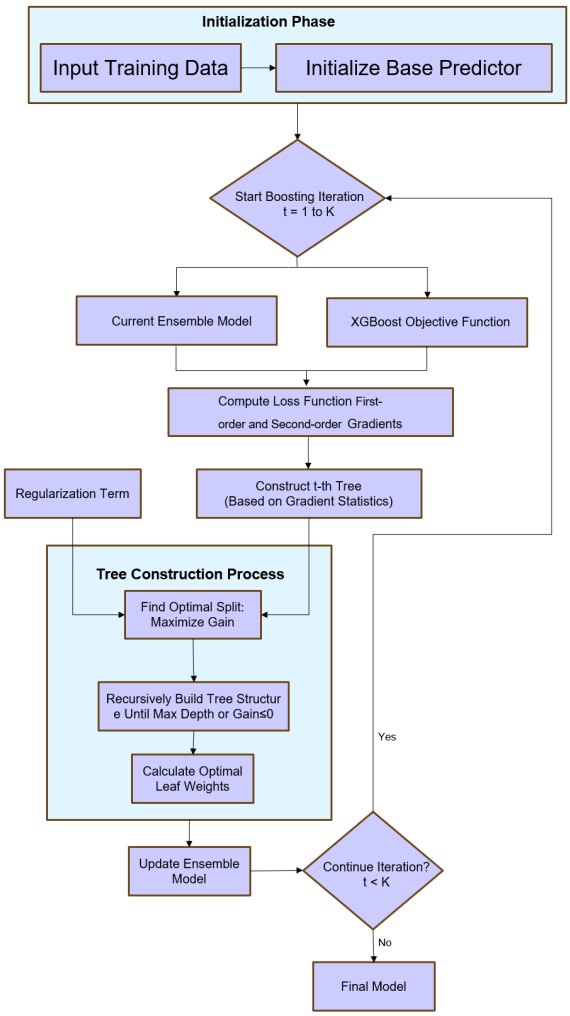

Figure 4. XGBoost algorithm workflow diagram.

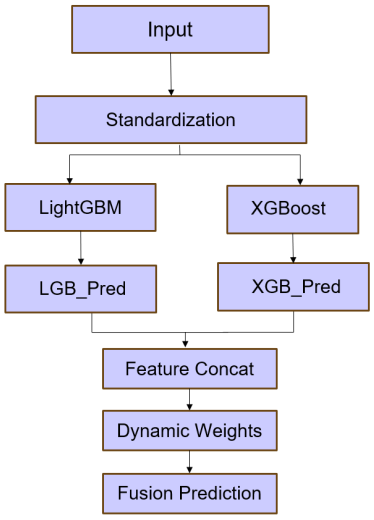

Figure 5. Enhanced Attention GBM workflow diagram.

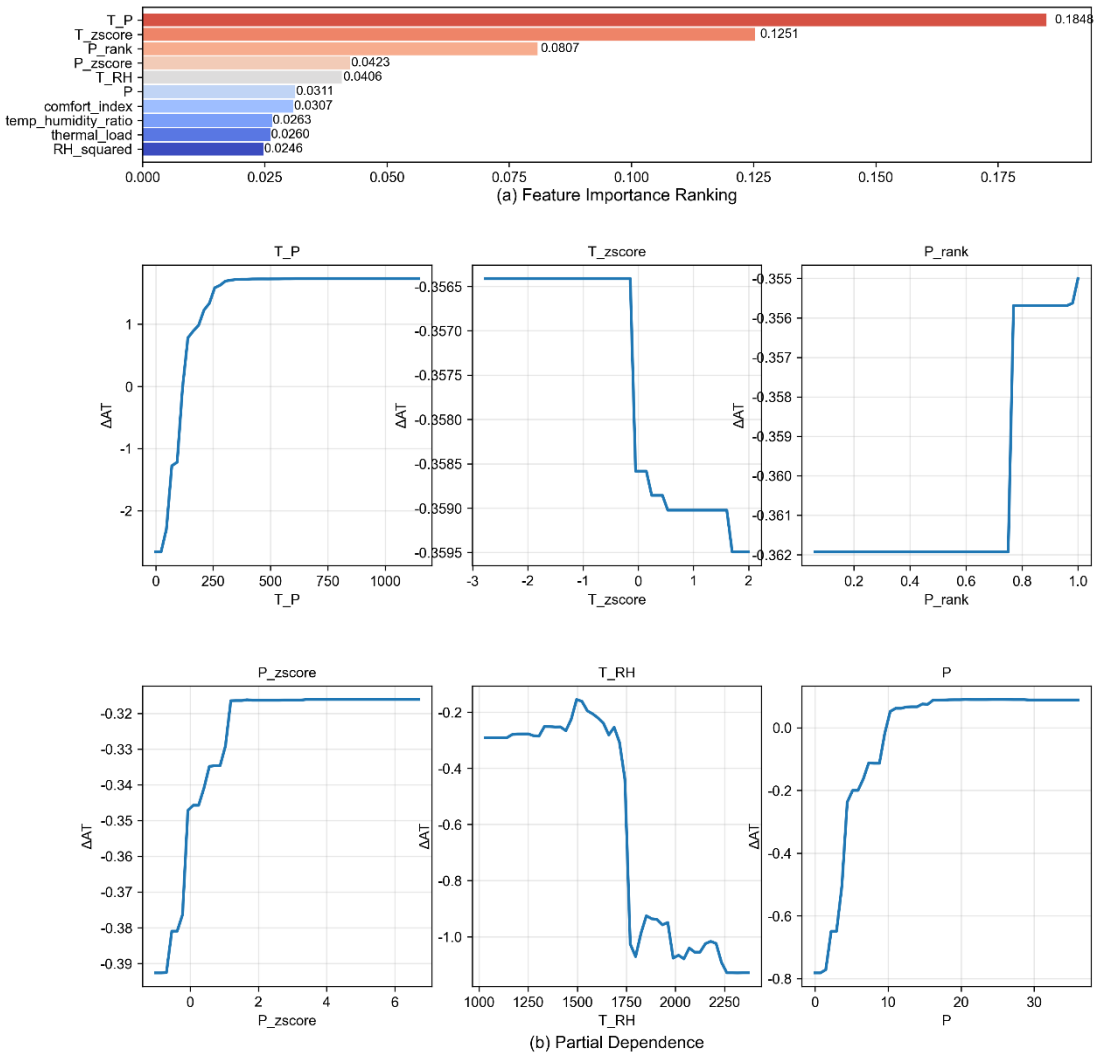

Figure 6. Interpretability analysis of the EAG.

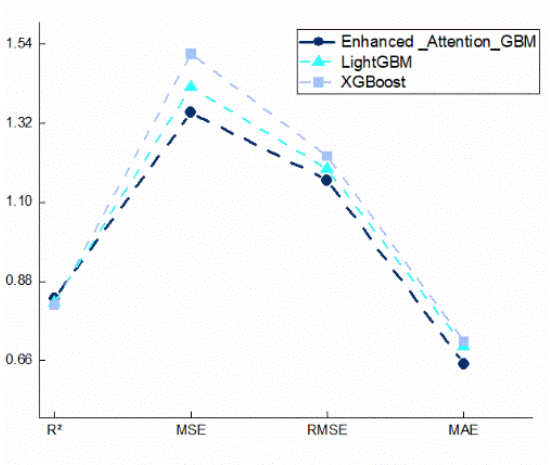

Figure 7. Performance metrics comparison.

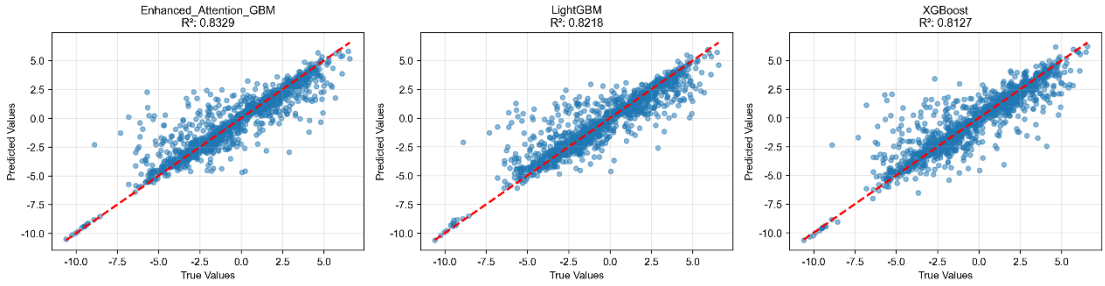

Figure 8. Model prediction comparison.

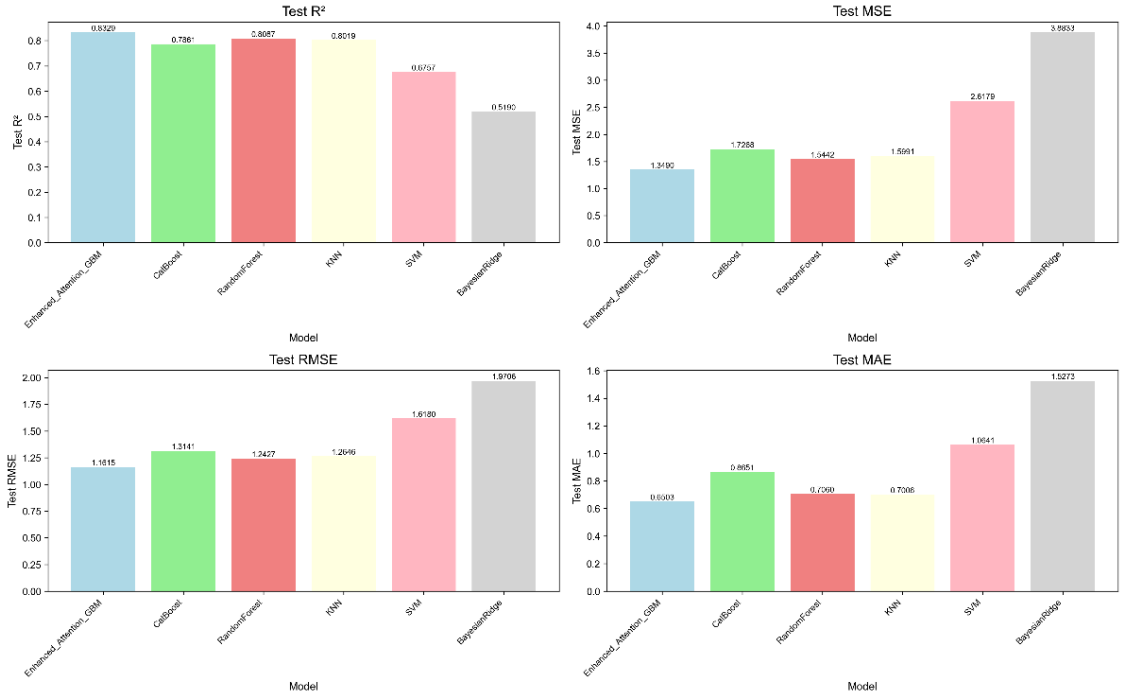

Figure 9. Comprehensive performance metrics comparison bar chart.

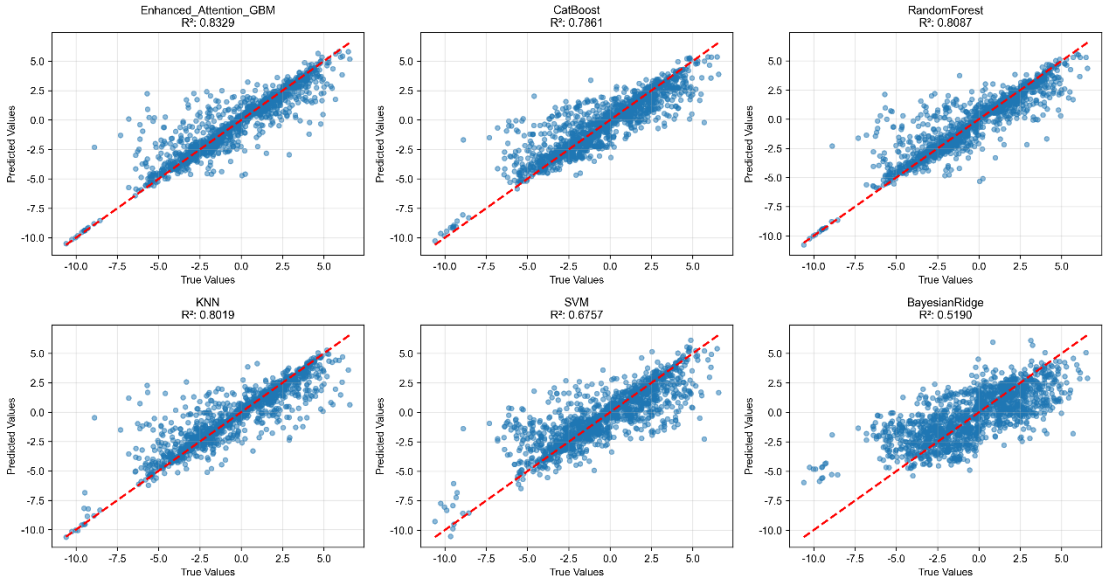

Figure 10. Model prediction effectiveness comparison chart.

Table 1. Description of raw data fields.

Field name	Unit	Description	Note
Timestamp	-	Date and time of data recording	Used for time-series analysis
T	°C	Ambient Temperature (Indoor Temperature)	Direct measurement
RH	%	Relative Humidity	Direct measurement
V	m/s	Air velocity at bird level	Direct measurement
A	days	Flock age	-
P	%	Real-time average panting rate of the flock based on computer vision	Behavioral indicator of heat stress

Table 2. Changes in each parameter with age.

Age (days)	RH_{target}	Wind chill coefficient	Wet-heat coefficient
1–6	60%	8	0.12
7–13	60%	6	0.12
14–20	55%	5	0.10
21–27	55%	4	0.08
28–24	55%	3.5	0.06
35–41	55%	3	0.03

Table 3. Experimental results of enhanced attention GBM.

R^2	MSE	RMSE	MAE
0.8329	1.3490	1.1615	0.6503

Table 4. Ablation study results comparison.

Models	R^2	MSE	RMSE	MAE
LightGBM	0.8218	1.4388	1.1995	0.7089
XGBoost	0.8127	1.5123	1.2297	0.7143
Enhanced Attention GBM	0.8329	1.3490	1.1615	0.6503

Table 5. A comprehensive performance comparison results.

Models	R^2	MSE	RMSE	MAE
Enhanced attention GBM	0.8329	1.3490	1.1615	0.6503
CatBoost	0.7861	1.7268	1.3141	0.8651
RandomForest	0.8087	1.5442	1.2427	0.7060
KNN	0.8019	1.5991	1.2646	0.7006
SVM	0.6757	2.6179	1.6180	1.0641
BayesianRidge	0.5190	3.8833	1.9706	1.5273